Energy 37 (2012) 207–219

Contents lists available at SciVerse ScienceDirect

Energy

journal homepage: www.elsevier.com/locate/energy

Application of exergy analysis in designing helium liquefiers

Rijo Jacob Thomas*, Parthasarathi Ghosh, Kanchan Chowdhury

Cryogenic Engineering Centre, Indian Institute of Technology, Kharagpur, West Bengal 721302, India

ARTICLE INFO

Article history:
Received 20 June 2011
Received in revised form
17 November 2011
Accepted 22 November 2011
Available online 20 December 2011

Keywords:
Helium liquefier design
Exergy analysis
Exergy destruction
Heat exchanger
Expander
Pressure drop

ABSTRACT

Exergy has proved to be a useful tool to analyze and optimize the design and operation of many systems. Some studies on helium refrigerators and liquefiers based on exergy are available in literature. In this paper, systematic evaluation of important operating and geometric parameters has been done to determine the exergy destructions in components as well as in the entire cycle of Collins helium liquefiers. Grassmann diagram of exergy flow has been shown to be of immense help in understanding relative importance of different components used in the system. Compressor pressure, expander flow rates, heat exchanger surface area are some of the parameters optimized considering both presence and absence of pressure drop in the heat exchangers. Non-dimensionalization of parameters makes the results applicable to plants of any capacity. Exergy-analysis based on Second Law proves to be far superior to the First Law based energy analysis in designing of the helium plant as the former is holistic in approach and capable of deriving some additional conclusions. Results derived on Collins cycle may be applicable in large-scale helium liquefiers by providing basic understanding of the influence of components on the plant performance and reasonable initial guess values in their design and simulation.
© 2011 Elsevier Ltd. All rights reserved.

1. Introduction

With recent developments in the area of high-energy physics, installations such as Particle accelerators, Colliders, Tokamaks etc widely came into being and as a result, the requirements for large-scale helium liquefaction plants also have increased. These helium plants are highly energy-intensive due to two reasons: (i) As the final refrigeration temperature is very low (normal boiling point of helium is 4.2 K), even the minimum theoretical power needed to remove every kilowatt of heat is very large, and (ii) the total quantity of heat (kW) to be removed from large installations (at 4.5 K and below) is usually very large. This makes the large helium plant a highly power-consuming device, where a savings of even a few percent by suitable design may make it an attractive proposition. Though energy efficiency stands out as the most desirable attribute to be taken up for maximization, there could as well be other objective functions, such as, weight, volume, reliability etc. to undertake studies for optimization of a helium plant. While designing helium plants, the system configuration as well as the component parameters such as efficiency of expander, effectiveness of heat exchangers, operating pressures of components, distribution of flow among the components etc., have to be properly selected to achieve the maximum possible efficiency. Thermodynamic irreversibility of the cycle, which is defined by the Second Law of Thermodynamics as entropy generation and loss of exergy (or useful work), provide a direct measure of the rate of liquefaction or capacity of refrigeration of a cycle. The major factors that contribute to the thermodynamic irreversibility are: heat transfer in heat exchanger across a finite temperature difference, other thermal irreversibility such as flow maldistribution, heat inleak and axial conduction in heat exchangers, pressure drop in piping and heat exchangers, isenthalpic expansion in Joule-Thomson valve, finite stages of compression, inefficiencies in expanders, inappropriate flow rates and operating pressures etc. In case of helium liquefaction cycles, the losses are distributed among different components throughout its operating temperature range, say 300 and 4.2 K. The amount of exergy remaining with the liquid output is a direct measure of the rate of liquefaction for a given input power (input exergy).

In order to reduce the thermodynamic irreversibility in the cycle, Collins [1] used expander- based cooling stages that replaced the LN_2 and LH_2 pre-cooling stages of the first helium liquefaction cycle by Kammerlingh Onnes [2]. Collins cycle is the basic cycle as far any commercial helium liquefaction system is concerned. Later, there have been modifications on this basic cycle, such as replacing the reciprocating engine-based expanders by turbines and arrangement of the turbines in series [3]. Wet expanders replaced JT (Joule-Thomson valves) [4] or expander-JT combinations have been employed as final liquefaction stage [5]. System efficiency has also been improved by adding more number of expander stages,

* Corresponding author. Tel.: +91 3222 281452; fax: +91 3222 282258.
E-mail address: rijojthomas@gmail.com (R.J. Thomas).

0360-5442/$ – see front matter © 2011 Elsevier Ltd. All rights reserved.
doi:10.1016/j.energy.2011.11.044

modifying arrangements of expanders to match the enhanced performances of compressors, expanders and heat exchangers [6] etc.

The present day large-scale helium liquefiers, therefore, have such features in their configurations which are similar, and at the same time, many others which are dissimilar to Collins Cycle. Thus, Collins cycle, which is composed of two reverse Brayton stages (henceforth referred to as refrigeration stages) as a cascade and a final JT or wet-expander liquefaction stage, still remains the basis for designing helium liquefaction cycles. A reverse Brayton stage consists of two heat exchanges and one expander, wherein the higher temperature heat exchanger is used for pre-cooling the working fluid before it is near-isentropically expanded in the expander and returns as cold low-pressure stream through the second heat exchanger. The lower temperature heat exchanger is used for absorbing the load which the reverse Brayton Cycle is meant to be used for. A large-scale helium liquefaction cycle is obtained by incorporating more number of refrigeration stages to the basic cycle. Therefore, the optimum values of operating and geometric parameters and their ranges obtained using Collins cycle may act as a guide in deciding the initial design values for large cycles. Determination of the number of refrigeration stages, arrangement the expanders, requirement of surface area for each heat exchanger in a large cycle have to be initiated from the results obtained from the analysis of Collins cycle. Adoption of this approach is thus expected to reduce the efforts of designing large-scale helium liquefier which has complex cycle configuration with large number of components, its performance being dependent on the geometric and operating parameters of these components.

Studies made by the authors based on First Law energy analysis brought out some of the optimum parameters for helium liquefiers in a Collins cycle [7–9]. However, the First Law is concerned only with the conservation of the quantity of energy and cannot determine the degradation in the quality of energy. Exergy-based analysis has the potential to identify the amount of thermodynamic irreversibility associated with the whole cycle as well as with each component. Thus, an optimization of any system can be performed by selecting the configuration, mass flow rates, operating pressures etc. such that they all contribute to the minimization or maximization of the objective function, namely, exergy destruction or exergy efficiency of the system respectively. In any liquefaction/refrigeration plant, there is no direct power input given to the cold box. Instead, it utilizes the exergy supplied by the compressor at the inlet to the cold box. Power is consumed in the compressor alone. The job of the cold box for a liquefier is an efficient utilization of the input exergy associated with high-pressure gas to get as high as liquid exergy (exergy associated with the amount of liquid produced) as possible. Exergy efficiency of the plant is thus defined as the ratio of liquid exergy to the exergy input to cold box. Reduced exergy destruction is manifested in terms of either increased liquid production or reduced power consumption (reduced input exergy) or both.

Earlier researchers have discussed the application of exergy analysis in evaluating certain other cryogenic processes [10–14]. A number of exergy studies have been reported in the literature on helium plants. Trepp [15] is a pioneer to apply exergy as a tool for the analysis of helium cycles. He discussed on the various exergy losses in cycles, particularly in heat exchangers and expanders. Thirumaleshwar [16] presented enthalpy–exergy diagram for helium and used the diagram to analyze a helium refrigerator based on reverse Brayton cycle. From his study, the distribution of exergy losses in main components of any helium liquefaction/refrigeration cycle such as, compressor, cooler, expander, heat exchanger etc, can be obtained. He also compared the exergy destructions due to pressure drop and due to finite temperature difference in a heat exchanger. Exergy analysis on different helium refrigerator cycles with more number of expanders provided the exergy destruction in the cycle components at various temperature levels [17–20]. Hubbell and Toscano [21] presented the losses at individual components for a two-expander helium liquefaction cycle and reported that more than 50% of the loss occurs at the compressor. They have also given the distribution of losses among different heat exchangers and other cold box components. These studies present estimations of component exergy destructions for different configurations of helium liquefaction cycles. However, as configuration of each cycle may change depending on application or objective function considered, exergy losses estimated and the optimum operating conditions determined for one cycle may not be directly applicable for the design or improvement of another cycle unless some correlations between them are established. It may also be observed that most of the studies have been made on helium refrigerators with only a handful among them on liquefiers and many optimum operating points for refrigerators may not be the same as those of liquefiers [22] due to important differences between them with regard to return mass flow rate and ultimate cold utilization.

1.1. Problem statement

From the review of literature, it is evident that there is still a need for detailed studies on Collins cycle using exergy as an effective tool whose results may easily be extrapolated and applied for generating the initial design-guidelines for large-scale helium liquefaction plants.

Therefore, this study attempts:

i) To explore the scope of using exergy analysis in optimizing Collins helium liquefaction system in terms of its operating pressure, mass flow rate diversion through expanders, heat exchanger surface area with and without the effects of pressure drop considered.
ii) To identify the aspects where exergy analysis is superior to the First law based energy analysis.
iii) To determine if there is a correlation in heat exchangers between the optimum surface area considering pressure drop and the saturation surface area without considering pressure drop.
iv) To determine the suitability of employing exergy analysis as a tool for the design of large-scale helium liquefaction plants.

The results obtained in this study are applicable for the particular system considered for analysis. However, Collins cycle has less number of components and thereby, less number of parameters to handle than a large-scale real helium plant does. It makes the analysis simpler and provides more clear understanding of the processes and of the effects of parameters on the overall plant performance. If the correlations between different parameters are established from the analysis of Collins cycle, it could well be extended as initial guess values for large-scale cycles. It is not possible to predict the exact optimal design in advance for a larger system based on the results of a smaller (less number of components) system. However, analyses on smaller systems may give a fair idea on the starting values of a more complicated system design often necessitating only fine-tuning, resulting in reduced time involved in the design and analysis. Therefore, although the results obtained from the Collins cycle may not be directly applicable to a large cycle per se, the trends are likely to give the designer a clear direction of improvement in terms of configuration and component efficiency that would result in further overall decrease of the loss of exergy in the processes involved. This approach may be more realistic than taking up large-scale helium liquefaction cycles for analysis right from the starting of the design process.

2. Methodology

An exergy based analysis has been performed on Collins helium liquefaction cycle. The schematic and the temperature-specific entropy (T-s) diagrams for the selected cycle have been shown in Fig. 1.

2.1. Assumptions

The study has been performed on the basis of the following assumptions:

1) The system is at steady state;
2) The efficiencies of components like compressor and expanders do not vary with pressure, temperature and mass flow rate;
3) Heat transfer coefficient of heat exchangers do not vary with pressure, temperature or mass flow rate.
4) Heat inleak and other thermal irreversibilities, such as axial heat conduction, flow maldistribution, non-counterflow configurational effect etc., have been taken into account in effective UA of heat exchangers.
5) The effects of heat inleak into the pipelines have been neglected.

2.2. Solution procedure

Collins cycle is dependent upon the components and operating parameters for its performance. The behavior of these parameters is intertwined and can be better understood with the use of process simulators. A commercial process simulator, Aspen HYSYS® V7.0, has been selected for the study. Process simulators usually have the flexibility of operation, capacity to produce results at a good speed and also have tools for performing sensitivity analysis, optimization studies etc. For generating the thermo-physical properties of helium in this simulator, the widely accepted 32-parameter modified BWR EOS (Equation of State) has been used [23].

2.3. Validation of the simulator

In order to validate the simulator, an actual plant has been simulated using Aspen HYSYS® V7.0 and the results of the simulation have been compared using the plant operation data which provides deviation of less than 1% [24,25]. The equipment models in Aspen HYSYS® V7.0 have been validated for a temperature range from 300 K to 2.2 K in helium plants by Deschildre et al. [26]. The simulation models have also been validated by checking the relative errors of mass and energy balances of each component and the entire system. The tolerances have been kept as: Temperature: 0.001 K, pressure: 0.0001 bar, flow rate: 0.0025 g/s, enthalpy: 0.01 W, entropy: 0.01 W/K, composition: 0.0001 and vapor fraction: 0.001.

2.4. Methodology for analysis

The general equation for exergy balance is written as:

$$\sum_j \dot{Q}_j\left(1-\frac{T_0}{T_j}\right)-\dot{W}+\sum_{IN}\dot{E}x_{FLOW}-\sum_{OUT}\dot{E}x_{FLOW}-\dot{E}x_{DEST}=0 \quad (1)$$

where, Term I represents the exergy transfer associated with the heat transfer, $\dot{Q}$ is the rate of heat transfer across a boundary (kW) where T_j (K) stands for any instantaneous temperature, T_0 (K) represents the temperature of reference state. Exergy transfer accompanying the work interaction (Term II) equals the electrical or mechanical work $\dot{W}$ (kW). Terms III and IV of the equation correspond to the exergy transfer accompanying the mass crossing the system boundaries at the inlet and outlet of any system.

Exergy transfer accompanying the mass flow is given as:

$$\dot{E}x_{FLOW} = \dot{m} \times ex \quad (2)$$

where, $\dot{m}$ represents the mass flow rate crossing the system boundaries, (kg/s); ex represents the exergy per unit mass flow, (kJ/kg) and is defined as; $ex=[(h-h_0)-T_0(s-s_0)]$. h and s correspond to the specific enthalpy and specific entropy of a fluid respectively. Similarly, h_0 and s_0 are the specific enthalpy and specific entropy respectively at the reference condition T_0 and P_0. For this case $T_0 = 300$ K and $P_0 = 1.013$ bar.

Exergy destruction, which is term V in Eq. (1), occurs due to thermodynamic irreversibility associated with the process and is expressed as:

$$\dot{E}x_{DEST} = T_0\dot{\Delta}S_{GEN}, \quad (3)$$

where $\dot{\Delta}S_{GEN}$ represents the rate of entropy generation (kW/K).

When the exergy balance equation given as Eq. (1) is applied to the control volume drawn across the cycle as shown in Fig. 1, it gives:

$$\dot{m}_{COMP}(ex_2-ex_{1'})=\dot{m}_L(ex_L-ex_{1'})+\dot{m}_{EXP1}(ex_3-ex_{11'})+\dot{m}_{EXP2}(ex_5-ex_{9'})+\dot{E}x_{DEST\_COLDBOX} \quad (4)$$

where, $\dot{m}_{COMP}$ and $\dot{m}_{EXP}$ are the rate of mass flows through compressor and the expander respectively (kg/s), $\dot{m}_L$ is the rate of liquid produced (kg/s), ex represents specific flow exergy values (kJ/kg) at various state points as marked in Fig. 1. $\dot{E}x_{DEST\_COLDBOX}$ denotes for the total exergy destruction in the cold box shown by the control volume drawn in Fig. 1.

Rearrangement of Eq. (4) gives:

$$\frac{\dot{m}_L}{\dot{m}_{COMP}}(ex_L-ex_{1'}) = (ex_2-ex_{1'}) - \frac{\dot{m}_{EXP1}}{\dot{m}_{COMP}}(ex_3-ex_{11'}) - \frac{\dot{m}_{EXP2}}{\dot{m}_{COMP}}(ex_5-ex_{9'}) - \frac{\dot{E}x_{DEST\_COLDBOX}}{\dot{m}_{COMP}} \quad (5)$$

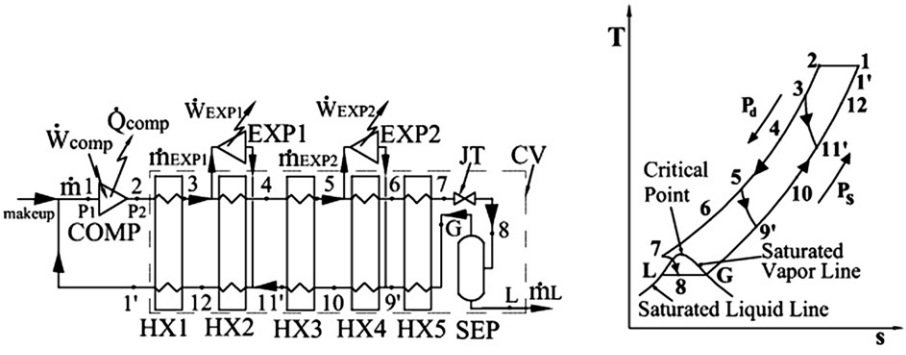

Fig. 1. Schematic and T-s diagrams of the Collins helium liquefaction cycle (Broken line encloses the control volume).

The liquid yield (y) on the basis of exergy may be written as:

$$y = \frac{\dot{m}_L}{\dot{m}_{COMP}} = \frac{ex_2 - ex_{1'}}{ex_L - ex_{1'}} - x_{EXP1}\frac{\Delta ex_{EXP1}}{ex_L - ex_{1'}} - x_{EXP2}\frac{\Delta ex_{EXP2}}{ex_L - ex_{1'}} - ex_{DEST\_COLDBOX} \quad (6)$$

where, $ex_{DEST\_COLDBOX}$ is the specific exergy destruction in all the components (except those of the expanders, which are taken care of in Term II and III on the RHS) inside the control volume as shown in Fig. 1 on the basis of total compressor flow, x_{EXP1} and x_{EXP2} are the fractions of compressor flow diverted through the expanders, Δex_{EXP1} and Δex_{EXP2} represent the change in specific exergy in the expanders.

Term I in RHS of Eq. (6) represents the contribution compressor towards liquid yield and is a positive quantity. Term II and III of RHS represent the exergy utilization in expanders EXP1 and EXP2, respectively. Finally, term IV in RHS stands for the exergy destruction in all components except that in the expanders. It may be noted that as the work produced by the expanders is not utilized in the cycle [27], the same has been shown as Term II and III of RHS.

It may be observed that all the terms in the RHS of Eq. (6) are positive quantities. While the term I on the RHS represents creation of exergy by the compressor $\dot{m}_{COMP}(ex_2 - ex_{1'})$, the terms II and III are the consumption of exergy in the expanders and term IV is the destruction of exergy due to the thermodynamic irreversibility in all components in cold box (except the expanders). This has been clearly depicted using the Grassmann diagram later. It may be noted that this concept of exergy utilization and destruction is unique to the Second law and cannot be brought out by the First Law based energy analysis.

When the energy balance is taken across the control volume drawn in Fig. 1 and the yield for Collins cycle is derived by Barron [28], it may be written that:

$$y = \frac{\dot{m}_L}{\dot{m}_{COMP}} = \frac{h_{1'} - h_2}{h_{1'} - h_L} + x_{EXP1}\frac{\Delta h_{EXP1}}{h_{1'} - h_L} + x_{EXP2}\frac{\Delta h_{EXP2}}{h_{1'} - h_L} \quad (7)$$

where, h represents for the enthalpy values at various state points as marked in the figure (kJ/kg), x_{EXP} stands for fraction of compressor flow through expander and Δh_{EXP} represents the enthalpy drop provided by the expanders (kJ/kg).

As a matter of comparison between energy and exergy analyses, it may be observed that Term I in the RHS of Eq. (7) which is considered as the compressor contribution to the liquid yield, is negative in the case of helium. Therefore, on the basis of the First Law based yield equation, the only contributors to liquid yield are term II and III which represent the work extraction (or refrigeration produced) in the expanders EXP1 and EXP2 respectively.

$$\text{Net exergy output of the cold box} = \dot{m}_L\,(ex_L - ex_{1'}) \quad (8)$$

$$\text{Net exergy input to cold box} = \dot{m}\,(ex_2 - ex_{1'}) \quad (9)$$

The above-mentioned exergy input is created by the compressor (COMP) which consumes a power of $\dot{W}_{COMP}$ (kW). Therefore,

$$\dot{W}_{COMP} = \dot{m}\,(ex_2 - ex_{1'}) + Ex_{DEST\_COMP} \quad (10)$$

where, Ex_{DEST_COMP} is the exergy destruction taking place in compressor.

Therefore, the exergy efficiency of the cold box may be defined as:

$$\eta_{Ex\_COLDBOX} = \frac{\dot{m}_L\,(ex_L - ex_{1'})}{\dot{m}\,(ex_2 - ex_{1'})} \times 100\% \quad (11)$$

The exergy efficiency of the compressor is defined as:

$$\eta_{Ex\_COMP} = \frac{\dot{m}\,(ex_2 - ex_{1'})}{\dot{W}_{COMP}} \times 100\% \quad (12)$$

where, $\dot{W}_{COMP}$ is the gross electrical work input to the compressor (kW).

However, in large helium cycles the expander work may be recovered and that will result in the reduction of $\dot{W}_{COMP}$ to the net power requirement $\dot{W}_{COMP\_NET}$ (kW):

$$\dot{W}_{COMP\_NET} = \dot{W}_{COMP} - \sum \dot{W}_{EXP} \quad (13)$$

where, $\sum \dot{W}_{EXP}$ (kW) is the sum of work of all the expanders in the cycle.

In the present case, however, the gross and the net work input to the compressor are the same as the expender work is not utilized.

Therefore, the overall exergy efficiency of the cycle is defined as:

$$\eta_{Ex\_CYCLE} = \eta_{Ex\_COMP} \times \eta_{Ex\_COLDBOX} = \frac{\dot{m}_L(ex_L - ex_{1'})}{\dot{W}_{COMP}} \times 100\% \quad (14)$$

Thomas et al. [29] has shown that Eq. (14) is the Figure of Merit or Carnot efficiency of a liquefaction cycle as proposed by Barron [28].

The exergy destruction in the cycle ($\dot{E}x_{DEST\_CYCLE}$) may be defined as the sum of exergy destructions in all its constituting components including the compressor. When $\dot{E}x_{DEST\_COLDBOX}$ stands for the total exergy destruction in the cold box (except the expanders) and $\dot{E}x_{DEST\_COMP}$ represents the exergy destruction in compressor.

$$\dot{E}x_{DEST\_CYCLE} = \dot{E}x_{DEST\_COLDBOX} + \dot{E}x_{DEST\_COMP} + \dot{E}x_{DEST\_EXP} \quad (15)$$

Overall exergy efficiency of the cycle may be defined in terms of the exergy destruction in the cycle as:

$$\eta_{Ex\_CYCLE} = \left[1 - \left(\frac{\dot{E}x_{DEST\_CYCLE}}{\dot{W}_{COMP}}\right)\right] \times 100\% \quad (16)$$

2.5. Parameters considered

The parameters considered for the study are compressor discharge pressure, mass flow through expanders, expander efficiency and added surface area to basic area of heat exchangers with and without the considerations of pressure drop.

The surface area requirement of a heat exchanger may be represented by effective UA which is the product of overall heat transfer coefficient (U) and the heat transfer area (A) of a heat exchanger taking into account all thermal irreversibility in a real heat exchanger, such as flow maldistribution, axial heat conduction through the metal as well as the process fluid, heat inleak, non-counter flow configuration effects etc. In other words, when inserted into an ideal counterflow equation relating effectiveness-NTU, effective UA would produce the actual effectiveness of a heat exchanger.

In the study, the effective UA of heat exchanger has been presented in non-dimensional form as 'Nondimensional effective UA'.

$$\text{Nondimensional effective UA} = UA/\dot{m}_{COMP}c_P \quad (17)$$

We assume U to be constant for all heat exchangers in spite of variations in mass flow rates and fluid properties. In the present definition of non-dimensional UA, it is always divided by a constant value which is the rate of heat capacity of the fluid at the suction of the compressor ($\dot{m}_{COMP}c_p$), where the mass flow rate and specific heat c_P are calculated at the compressor suction condition of 300 K

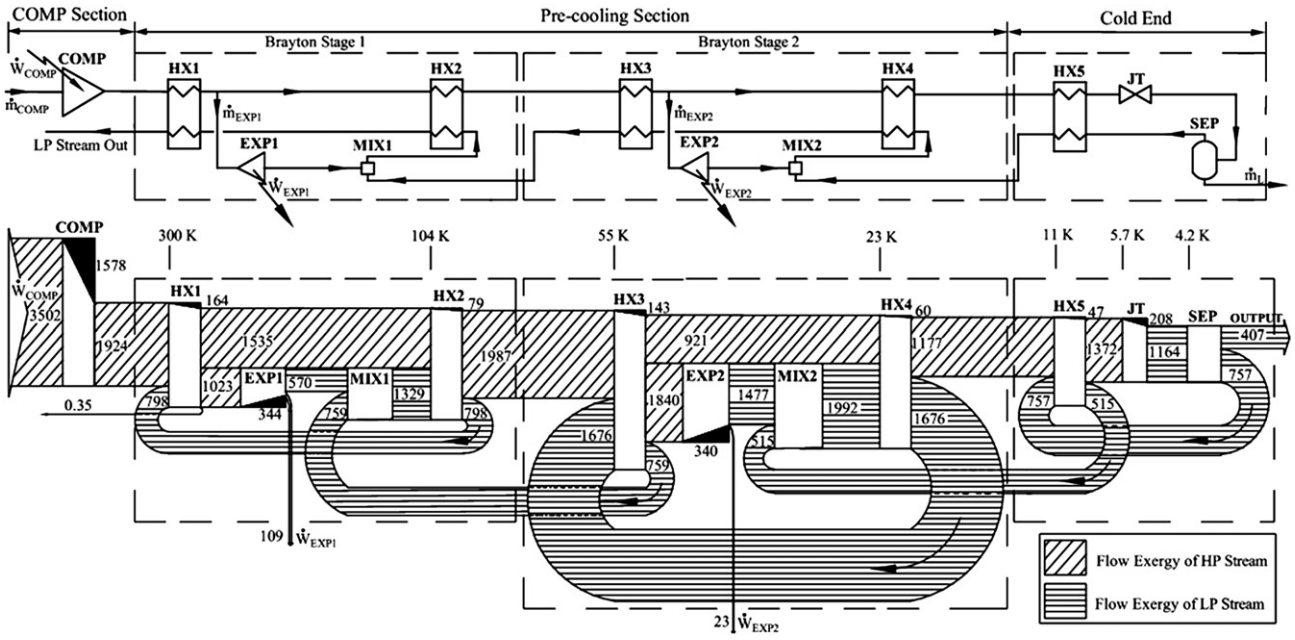

Fig. 2. Grassmann diagram for Collins helium liquefaction cycle for a selected operating condition [P_s = 1.01 bara, $\eta_{Isothermal\_COMP}$ = 55%, $\eta_{EXP1} = \eta_{EXP2}$ = 70%, $\dot{m}_{EXP1} = \dot{m}_{EXP2} = 0.4\dot{m}_{COMP}$, $\varepsilon_{HXs} = 0.97$] [Broken lines enclose control volumes].

and atmospheric pressure. This non-dimensionalization allows one to use the results obtained in the present analysis to design helium liquefaction plants of any capacity.

As one parameter is varied, other parameters have been kept constant at certain 'base values' which are as follows: Efficiency of each of the expanders, $\eta_{EXP1} = \eta_{EXP2}$ = 70%, Fraction of total compressor mass flow diverted through each of the expanders $\dot{m}_{EXP1} = \dot{m}_{EXP2} = 0.4$, Effectiveness of each of the heat exchangers, $\varepsilon_{HXs} = 0.97$. The suction pressure of the compressor has been kept atmospheric, P_s = 1.01 bara. The isothermal efficiency of the compressor is 55%, which is expected for oil-injected screw compressors, when a compression process has 3 stages of equal pressure ratios and the same inlet temperature of 300 K for all stages [30]. The final discharge pressure of the compressor has been kept at $P_d = 22$ bara. The effects of each of the selected parameters on exergy destruction and/or exergy efficiency are presented for the components, the cold box as well as for the whole cycle.

2.6. Exergy analysis and thermoeconomics

Exergy analysis of a system aims at maximizing the exergy output of a system for a given exergy input, or in other words, the exergy efficiency needs to be maximized. In order to achieve this objective, exergy destruction at each component has to be minimized, which often calls for increasing thermal and hydraulic efficiency of individual component and process. This, in turn, demands increase of design and input cost. For example, exergy destruction in a heat exchanger can be reduced by decreasing the temperature difference among fluids by increasing heat exchanger surface area. However, this would increase the capital investment of the plant. Exergy loss arising from the pressure drop in a pipeline can be reduced by increasing the diameter and smoothness of the tube, which again calls for increasing the investment. An increase in efficiency of expander would reduce exergy destruction. However, it would require sustained investment in design improvement and consequent associated cost.

As the exergy is the input and output parameters in thermodynamic analysis of a system based on exergy, it is possible to assign a cost (in terms of capital, operating and maintenance cost) per unit of exergy associated with input and output of each component, sub-system or the whole system. This approach, called Thermoeconomics based on exergy analysis or "Exergoeconomics" would help to design a plant based on cost consideration. In this way, the thermodynamic performance of a system can be evaluated along with the cost involved [31].

2.7. Grassmann diagram for Collins cycle

Only a little more than half of the work input to compressor is utilized by the compressor in increasing the level of exergy from the state of its input to the output. The output exergy from the compressor is the input exergy to the cold box and majority portion of this exergy is lost in various components due to thermal irreversibility and pressure drop. Only a small portion of this input exergy is obtained back as expander work, which, in majority of the cases, is not utilized in the cycle. The remaining exergy that comes out of the cold box is output exergy which is the flow exergy associated with the liquid withdrawn. The Grassmann diagram is a graphical representation of the flow of exergy in any system and therefore, is also known as the exergy–flow diagram. It illustrates how a part of the input exergy supplied to a system is destroyed (or utilized) in the successive stages of the processes. It gives various exergy interactions in the system as well as the input–output relationships among the components inside the system showing the destruction of exergy (loss). Thus Grassmann diagram provides a clear understanding about the processes and a direction to improve the performance. It may be very useful in understanding helium liquefiers where stream splitting, mixing and recirculation make the system quite complex [32].

2.7.1. Method of construction

The Grassmann diagram for Collins helium liquefaction cycle, which operates between a wide temperature range of 300 K - 4.2 K with a number of re-circulating streams, has been generated and shown in Fig. 2. Corresponding schematic diagram of the selected

cycle is also shown. Broken lines have been used to enclose the control volumes. Contrary to Fig. 1, control volumes have been drawn around 3 sections of the cycle in Fig. 2. The first two sections include two heat exchangers and one expander each and are called pre-cooler stages. The last section contains one heat exchanger and the Joule-Thomson valve, called liquefaction stage or Joule-Thomson stage (Cold End). The following steps have been performed to generate the diagram:

Step 1: For a selected operating condition, flow exergy values at various state points of the cycle as well as the work and heat interactions have been calculated.
Step 2: The input as well as the output exergy of each component have been found and exergy balance has been applied to calculate the exergy utilization and/or destruction in each component.
Step 3: The width of each exergy flow has been drawn proportional to its magnitude. In order to distinguish between the exergy associated with the HP (high-pressure) streams and that with the LP (low-pressure) streams, they are shaded differently.
Step 4: In the diagram, the white portions indicate the components and the exergy destruction taking place inside each component has been shaded as black. It may be noted that in the diagram the input to any component is on its left side and output on the right side. The recycle streams that flow from right to left have been shown with a return arrow.
Step 5: Grassmann diagram starts with the exergy addition in the compressor station (COMP) where power is consumed. COMP in the diagram represents a multistage compressor system with inter-coolers and after-cooler. The total exergy destructions taking place in all the components inside the compressor station together is marked as the exergy destruction in COMP.
Step 6: For the heat exchangers (HX1 to HX5), the exergy is supplied by both HP and LP streams and therefore, they are shown on the left side of each HX block in the diagram. Similarly, in the outlet both the HP and LP streams carry away the exergy and have been shown on the right side.
Step 7: In case of the expanders EXP1 and EXP2, a part of the input exergy is converted to useful works and have been separately marked in the diagram. They are shown to have exited the control volume.
Step 8: There is no work production by JT and only the input and output exergy flows are marked for Joule-Thomson stage (Cold End).
Step 9: The exergy destruction due to mixing in the mixers MIX1 and MIX2 are negligible and are not shown in the diagram. Similarly, the exergy destruction in the phase separator (SEP) is also negligible.
Step 10: The final output of the cycle, which is the exergy associated with the liquid drawn, is shown at the end of the diagram on the extreme right.

3. Results and discussions

3.1. Exergy expenditure in Collins cycle on the basis of Grassmann diagram

The following observations may be made from Fig. 2:

- More than 88% of the input exergy or the power supplied to the cycle has been dissipated in the different components and only less than 12% is available as the output liquid exergy.
- Out of all the components, exergy destruction is the highest in COMP (45%). Therefore, the exergy supplied to the cold box after the isothermal compression process is only about half of compressor power input. It may be noted that the exergy efficiency of isothermal compression process is the same as the isothermal efficiency of the compressor which has been specified as 55% for the simulation.
- In ranking of exergy destruction, expanders come next to the compressor in the cycle. More than 20% of the supplied exergy to cold box is destroyed in two expanders. Though operating at different temperature levels, the exergy destructions in both the expanders are almost equal (10% each). It may be noted that exergy destruction occurs in expanders due to deviations from 100% isentropic efficiency. For this study, both the expanders have the identical isentropic efficiency of 70% and, consequently, the same exergy destructions. As the work of expanders is not utilized in the cycle, total exergy loss in expanders increase to about 23%.
- Though, the flow through the JT is only half of that through an expander, about 6% of the supplied compressor work is lost as exergy destruction in JT and this shows that it is a highly irreversible component. The exergy is destroyed in JT due to isenthalpic expansion of gas through the valve restriction. It may be observed that the exergy destructions in mixers (MIX) and, phase separator (SEP) have been considered to be negligible.
- Sum of the exergy destroyed in all the five heat exchangers together constitutes about 14% of the total supplied power. Out of this, 60% occurs in HX1 and HX3 together. HX1 and HX3 are the heat exchangers whose HP stream outlets are the inlet flows to EXP1 and EXP2 respectively. The exergy losses in HX2, HX4 and HX5 are comparable, with HX5 contributing the least. Exergy destruction in heat exchangers occurs due to two factors: i) heat transfer across finite temperature difference and ii) pressure drop. Wide difference between hot and cold streams temperatures at any point in heat exchangers occurs due to finite *UA* and/or due to imbalance in the heat capacity rates of the streams. The Grassmann diagram shows only the exergy destruction due to heat transfer across finite temperature difference. The effect of pressure drop on heat exchanger performance, however, is presented in a later subsection.
- Improvement of exergy of HP flow is obtained by utilizing the exergy associated with returning (or the re-circulated) LP streams which are outlet streams from expanders and the JT. The amount of exergy associated with the HP stream at the inlet of JT determines the output of pre-cooler stages.

3.1.1. Discussions on utility of Grassmann diagram

With the aid of Grassmann diagram, the role of each component of the cycle viz. compressor, expanders, heat exchangers, JT etc. and also the interactions between them are clearly depicted. Since the First Law is concerned about the conservation of energy, a similar heat flow (energy flow) diagram for cold box would have equal width throughout and would not reveal the thermodynamic irreversibility that is evident in the Grassmann diagram based on exergy flow. Different methods may be attempted to reduce the exergy destructions in the components of the cycle. It is apparent that the improvement in component efficiency reduces the exergy destruction in the component. However, there are always practical limits in achieving very high efficiencies of components and in many cases the operational parameters or the configuration may have to be optimized to reduce the total exergy losses of the system.

3.1.2. Compressor

Increasing the number of compression stages with inter-coolers and after-coolers increases isothermal efficiency and reduces

exergy losses in the compressor. Another possibility of reducing the exergy loss in compression process is by performing it at lower temperatures, for instance, at 80 K using liquid nitrogen pre-cooling. Practical aspects of developing a 80 K cold compressor have been reported in the literature [33].

3.1.3. Expander

In spite of the difference in operating temperatures, the exergy destructions in the expanders are almost equal, and this shows the need to design them to be equally efficient. In larger plants, where the expanders produce significant amount of work, the work may be recovered from expanders to reduce the net work requirement of cycle. However, it may be noted that even if it is utilized, it will not improve the exergy efficiency of cold box (as the extracted expander work exits the control volume of the cold box). However, it would increase the overall exergy efficiency of the cycle. The replacement of Joule-Thomson valve by less irreversible components like expanders would reduce the exergy loss. For Collins cycle, the improvement in rate of liquefaction with replacement of JT with expander is expected to be about 30% [4].

3.1.4. Heat exchanger

It has been observed from the Grassmann diagram that about 14% of the supplied power (exergy) is lost in the HXs as exergy destruction. In case of heat exchangers, even in the ideal ones with zero temperature of approach (which corresponds to the First Law efficiency of 100% for HXs), substantial exergy is lost due to the difference of temperatures between the fluids. The gap in the temperature profile occurs due insufficient heat transfer area and due to unequal heat capacity rates for the heat exchanger streams. Therefore, improvement of exergy efficiency in heat exchangers may be accomplished by: i) Addition of more heat transfer area and ii) Matching of heat capacities by adjusting the rate heat capacity of fluid streams. Addition of surface area to HXs improves the effectiveness of HXs and brings the temperatures closer so as to obtain zero temperature of approach. The second option may be accomplished either by changing the operating pressure of the streams (which changes the specific heat) or by adjusting the mass flow rates of the HX streams. The detailed exergy analysis on the heat capacity imbalance in helium liquefaction system has been published in reference [29]. The variation of specific heat is particularly significant in HXs working below 10 K. A change in the configuration of large-scale plants involving arrangements of the expanders and increasing the number of refrigeration stages would alter the ratios of mass flow rates in heat exchangers and reduce the exergy losses. It is also important to ensure that there is no temperature-cross inside the heat exchanger causing a violation of the Second Law of Thermodynamics.

Thus, Grassmann diagram grades the components in terms of their exergy losses and reveals their potentials in improving the overall performance of the entire system through exergy analysis and reduction of the exergy losses in them.

3.2. Effect of variation in compressor discharge pressure on cycle performance

Compressor discharge pressure (P_d) determines both the thermodynamic performance and the energy requirement of the cycle. In this section, P_d has been varied within a wide range of pressures between 4 and 34 bara and its effects on exergy efficiencies of compressor, cold box and cycle have been presented in Fig. 3.

The following observation may be made from Fig. 3:

- Exergy efficiency of the compressor is almost constant at 55% at all the pressures. It may be noted that for the simulation, the isothermal efficiency of the compressor has been kept constant at 55%. The isothermal efficiency of a compressor is the same as its exergy efficiency.
- The exergy efficiency of the cold box increases with increasing compressor discharge pressure up to 22 bara and deceases beyond it. Exergy efficiency of the cycle which is the product of exergy efficiency of cold box and compressor, therefore, follows a similar trend as that of cold box (as the exergy efficiency of compressor is constant).
- There is a sharp reduction in exergy efficiency when compressor discharge pressure exceeds 28 bara. As the pressure increases beyond 28 bara, the condition (T & P) of the inlet stream to JT becomes such that the isenthalpic expansion in JT results in reduced liquefaction which in turn affects the exergy efficiency of the cold box as well as the cycle.

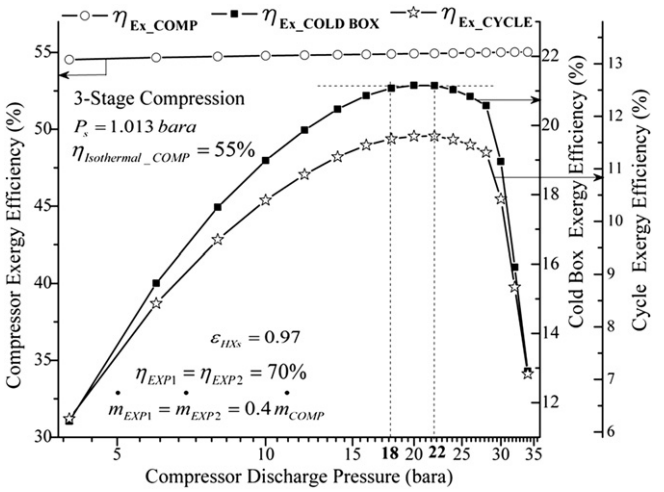

Fig. 3. Effect of variation of compressor discharge pressure on the cycle performance [P_s = 1.013 *bara*,η_{COMP} = 55%$\dot{m}_{EXP1} = \dot{m}_{EXP2} = 0.4\dot{m}_{COMP}$, $\eta_{EXP1} = \eta_{EXP2}$ = 70%, 3 Stage compression, each stage has the same pressure ratio and inlet temperature].

It may be concluded that there is a range for compressor discharge pressure, within which the cycle may be operated. For the selected configuration, maximum exergy efficiency is obtained at P_d between 18 and 22 bara. The First Law based energy analysis on Collins cycle also yielded similar results [7]. It may also been seen that many of the practical large-scale helium liquefaction plants operate between 18 and 22 bara [34–37]. Therefore, while designing large-scale helium liquefaction plants, a compressor discharge pressure of about 22 bara may be considered as a good initial estimation. The design pressure for a practical system may be fine-tuned on the basis of the performance of practically available compressors, expanders etc. and also on the economic considerations.

3.2.1. Effect of compressor discharge pressure on exergy destructions in components

Variation in compressor discharge pressure is expected to change the performance of each component and consequently, the exergy destruction in each of them. The variations in output exergy, expander work and the exergy destruction in all the cold box components with increasing compressor discharge pressure have been presented as percentage of total gross exergy input to the cold box (Fig. 4). The exergy destructions in other components of the cold box being negligible, the sum of the exergy destructions in HXs, EXPs, JT, along with the expander work and the output liquid exergy constitutes the total exergy input to the cold box. Therefore, along any vertical line, the sum of the Y-values of the curves is 100%.

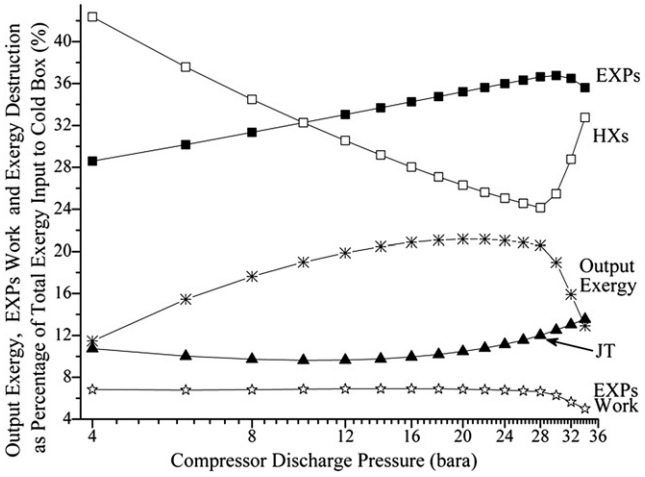

Fig. 4. Output exergy, work expanders and exergy destruction in the cold box components as percentage of total exergy input to cold box [P_s = 1.01 bara, $\eta_{Isothermal\_COMP} = 55\%$, $\eta_{EXP1} = \eta_{EXP2} = 70\%$, $\dot{m}_{EXP1} = \dot{m}_{EXP2} = 0.4\dot{m}_{COMP}$, $\varepsilon_{HXs} = 0.97$].

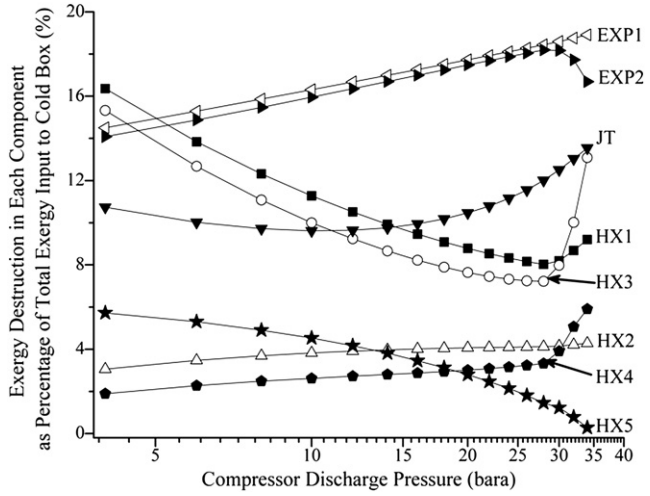

Fig. 5. Exergy destruction in each components as percentage of total exergy destruction in cold box [P_s = 1.01 bara, $\eta_{Isothermal\_COMP} = 55\%$, $\eta_{EXP1} = \eta_{EXP2} = 70\%$, $\dot{m}_{EXP1} = \dot{m}_{EXP2} = 0.4\dot{m}_{COMP}$, $\varepsilon_{HXs} = 0.97$].

The following observations may be made from Fig. 4:

- The exergy destructions in heat exchangers and expanders have opposing trends. As P_d increases (up to 28 bara), the exergy destruction in HXs decreases and that in EXPs increases. At compressor discharge pressures less than 10 bara, heat exchangers are the most exergy destructive component. At pressures above 10 bara, expanders surpass the heat exchangers as the most exergy destructive components. For any given P_d, the total exergy destruction in HXs and EXPs together is always more than 60% of the exergy input to cold box.
- The variation in exergy destruction in JT is comparatively less; however, the performance of JT becomes at its best at P_d near 10 bara. With further increase in P_d, the exergy destruction in JT increases. Therefore, JT pressure should preferably be about 10 bara.
- The sum of the work output from the expanders remains almost constant with increase in P_d up to 28 bara.
- Keeping other constraints in consideration, the compressor discharge pressure of cycle may be selected such that the output exergy is as high as possible. Taking into account the variations in each quantity, there is noticeable improvement in the output exergy with increase of P_d up to 28 bara. This finding has also been brought out from a detailed study on energy analysis [7].

Exergy destruction in each component is presented as percentage of the total exergy input to cold box and its effect on the variation of P_d has been plotted against a logarithmic scale in the *x*-axis as shown in Fig. 5. Exergy losses in each component of the cycle may provide a better understanding on the effects of compressor discharge pressure.

The following observations may be made from Fig. 5:

- With increase in compressor discharge pressure up to 28 bara, the exergy destruction in HX1, HX3 and HX5, which determine the inlet temperature to expansion devices, decreases. For EXP1, EXP2, HX2 and HX4 the exergy destruction increases. For JT, its exergy destruction increases significantly beyond $P_d = 10$ bara.
- The rate of decrease in exergy destruction in HX1 and HX3 is higher than the rate of increase in HX2 and HX4. The exergy loss in HX5 decreases substantially with increase in P_d. Total exergy loss in all HXs together decreases with increase in P_d up to 28 bara (as it has been seen in Fig. 4).
- Both the low and high temperature expanders (EXP1 and EXP2) have almost equal exergy destructions between 4 and 28 bara. This may also be observed in Grassmann diagram.
- Flow through JT is only half of that through an EXP ($\dot{m}_{EXP} = 0.4\dot{m}_{COMP}$ and $\dot{m}_{JT} = 0.2\dot{m}_{COMP}$). Yet, the exergy destruction in JT is comparable to that in expanders (for instance, at 28 bara, destruction is 12% for JT and 18% for EXPs. This proves the fact that JT is a highly irreversible component.
- When the compressor discharge pressure is at its optimum value of $P_d = 22$ bara, arrangement of components in the decreasing order of exergy destruction is: EXP1, EXP2, JT, HX1, HX3, HX2, HX4 and finally HX5.
- For all components, except the very low temperature components of JT and HX5, the variations of exergy destructions in components are almost linear in the semi-log graph. indicating that the variations are almost proportional to logarithm of compressor discharge pressure.

JT is an inherently irreversible component and the variation in exergy losses in JT is not proportional to the logarithm of P_d. In HX5, apart from the imbalance in mass flow rate, the exergy loss is also due to the heat capacity mismatch which arises from the imbalances in specific heat values of the heat exchanger streams. It may be noted that at low temperatures (where HX5 is operating), specific heat of helium is a strong function of temperature as well as pressure [29].

3.3. Combined effect of variations in expander flow and compressor discharge pressure

3.3.1. Optimum fraction of compressor flow diverted through expanders

Apart from the compressor discharge pressure, another important factor that decides the cycle performance is the amount of compressor flow diverted through the expanders. The optimum flow that has to be passed through the expanders is difficult to predict as it is dependent on a number of interdependent parameters.

In a heat exchanger, as depicted by the Grassmann diagram, the exergy of the HP forward stream increases by utilizing the exergy of the return LP stream. However, as more flow is diverted through EXP, the amount of exergy associated with the return LP stream

increases and the exergy associated with the input HP stream to HX decreases. Depending on the amount of the diversion through the expanders, it may lead to a net decrease of HP output exergy. As the exergy associated with the inlet stream to JT determines the liquid output, a higher exergy output from the last heat exchanger HX5 would increase the liquid yield of the plant. This may be accomplished by optimizing the widths of the recirculation streams (amount of the exergy re-circulated) at each temperature levels as shown in the Grassmann diagram. The optimum expander flow is also influenced by the variation in compressor discharge pressure. Therefore, the combined effect of expander flow and P_d has been studied and is depicted in Fig. 6. When varying the total expander flow, the flow through each expander is kept equal.

The following observations may be made from Fig. 6.

- With increase in flow through expanders from 70% to 90%, the maximum exergy efficiency for the cold box is obtained when 80% of the compressor flow is diverted through the expanders.
- For each expander flow, there exists a particular value for P_d that gives the maximum exergy efficiency. The optimum P_d values are about 24 bara, 22 bara and 14 bara for expander flow rates of 70%, 80% and 90% of the compressor flow respectively.
- When 90% flow is diverted through EXPs, the optimum compressor discharge pressure decreases to 14 bara with a decrease of the value of corresponding maximum exergy efficiency. Similarly for 70% EXP flow, the optimum P_d increases to 24 bara. Therefore, for a given configuration, there is a combination of pressure and expander flow that provides the maximum exergy efficiency for the cold box.
- Exergy efficiency is very sensitive to compressor discharge pressure when expander flow rate is more than the optimum value of 80%. The curves for 70% and 80% expander flow rates are flatter near its peak when compared to the 90% case.

The optimum expander flow diversion of 80% has also been found using the energy analysis [7]. This implies that 20% of the compressor flow should pass through the final liquefaction stage. When increasing both compressor discharge pressure and total expander flow beyond their optimum values, there is sudden drop in exergy efficiency and this shows the importance of the careful selection of operating parameters while designing any helium liquefaction plant.

3.3.2. Optimum flow requirement for each expander of the cycle

When the effects of compressor discharge pressure and total EXP mass flow have been calculated, the flow through each expander has been kept equal. A study has been performed to understand the effects of unequal flow through each of the expanders and thereby, to find the optimum flow through them. The total expander flow has been kept at the optimum total EXP flow of 80% of the compressor flow. The cycle performance with variations in compressor discharge pressure for 5 different flow distributions between EXP1and EXP2, which are 30%–70%, 40%–60%, 50%–50%, 60%–40% and 70%–30%, have been shown in Fig. 7.

The following observations may be made from Fig. 7:

- The maximum cold box exergy efficiency is obtained when the total expander flow is equally divided between the EXP1 and EXP2 (50%–50% case). However, there is no appreciable reduction in the cold box exergy efficiency with 10% variations from the 50%–50% case (40%–60% and 60%–40% cases).
- There is no change in the optimum operating pressures for the cycle (P_d = 18 - 22 bara) with variations in the distribution of flow between the expanders.

An earlier study based on the first law also found that the maximum performance is obtained when the total expander flow is equally distributed among the EXPs [7].

3.4. Effect of expander flow on exergy destruction in components

Change in mass flow rates through expanders alters the exergy destruction in each component in cold box and this has been plotted in Fig. 8. Exergy destruction in each component has been presented as percentage of total exergy input to the cold box.

With increase in expander flow beyond the optimum value of 80% compressor flow, there is a sudden increase in the total exergy destruction in the cold box (sum of exergy destructions in all the cold box components).

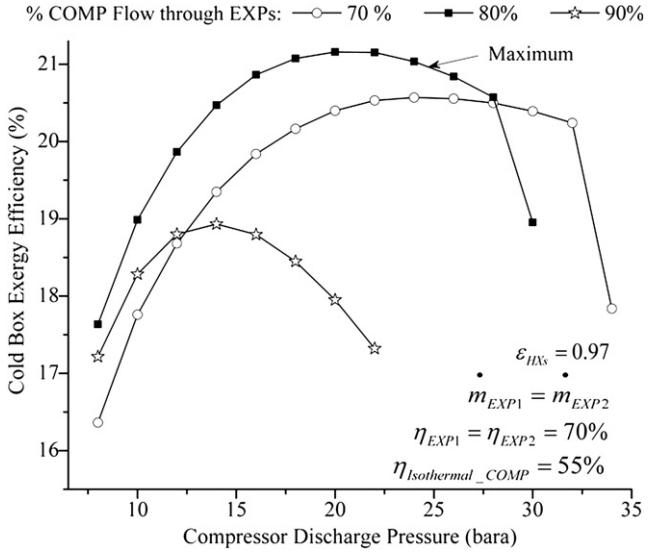

Fig. 6. Effects of variation of compressor discharge pressure on cycle performance for various expander flows [P_s = 1.01 bara, η_{COMP} = 55%, $\eta_{EXP1} = \eta_{EXP2}$ = 70%, $\dot{m}_{EXP1} = \dot{m}_{EXP2}$, ε_{HXs} = 0.97].

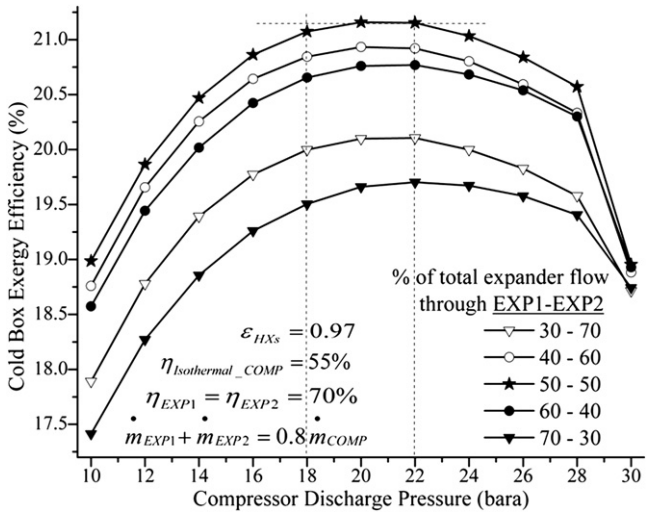

Fig. 7. Effects of variation of compressor discharge pressure on the optimum flow through each expander [P_s = 1.01 bara, η_{COMP} = 55%,$\eta_{EXP1} = \eta_{EXP2}$ = 70%, $\dot{m}_{EXP1} + \dot{m}_{EXP2} = 0.8\dot{m}_{COMP}$, ε_{HXs} = 0.97].

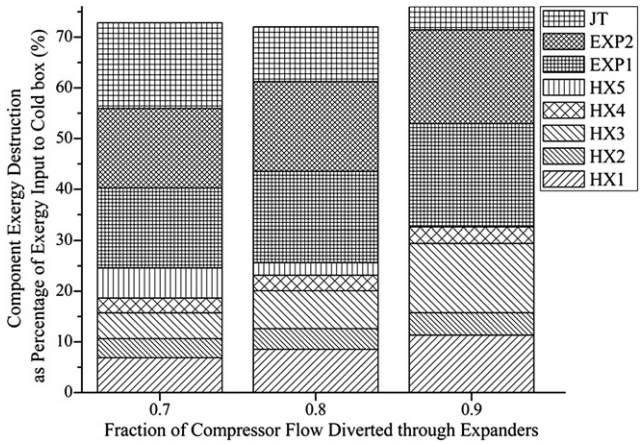

Fig. 8. Effect of variation in flow through expanders on exergy destruction in cold box components [P_s = 1.01 bara, $\eta_{Isothermal\_COMP}$ = 55%, η_{EXP1} = η_{EXP2} = 70%, $\dot{m}_{EXP1} = \dot{m}_{EXP2}$, ε_{HXs} = 0.97].

- With increase in flow through EXPs, the exergy destruction in both expanders, EXP1 and EXP2 increases proportionally. When increasing the flow through expanders, the flow through JT decreases and there is almost a proportional decrease in JT exergy loss.
- The increase in exergy loss in HX1 and HX3, which decide the inlet temperature to expanders EXP1 and EXP2 respectively, are very significant when compared to the other HXs.
- Exergy destruction in all HXs, except HX5, increases with increase in EXP flow. With increased expander flow, there is a significant reduction in the loss in HX5 which is due to the reduction in JT flow. When JT flow becomes only 10% of the compressor flow, the exergy destruction in HX5, therefore, is almost negligible.

It may be concluded that with increase in expander flow beyond the optimum value of 80% compressor flow, the exergy destructions in those heat exchangers which decide the inlet temperature to expanders increase substantially and this in turn increases the total exergy destruction in cold box.

3.5. Effect of variation in expander efficiency on the exergy efficiency

Apart from the expander mass flow, efficiency of expander is also expected to have a significant impact on the performance of liquefaction cycles. In order to study its impact on the exergy efficiency of the cold box, expander efficiency is varied within a practically possible range, 50–85% as shown in Fig. 9. While varying the isentropic efficiency of one expander, the other is kept constant at 70%.

It may be observed from Fig. 9 that the isentropic efficiency of expander has almost linear relationship with cold box exergy efficiency. When comparing the slopes, variations in isentropic efficiency of EXP1 and EXP2 have almost similar influence on exergy efficiency. This results helps to conclude that the expanders that operate at different temperature levels have almost equal importance. Detailed expander studies based on the First Law also brought out similar results [7,8].

It has been seen from the Grassmann diagram that a significant amount of exergy input to cold box is destroyed in the heat exchangers. Therefore, the final output of the helium cycle, to a large extent, depends on the performance of the heat exchangers. When performing the parametric studies discussed in the previous subsections, the effectiveness of the heat exchangers are kept

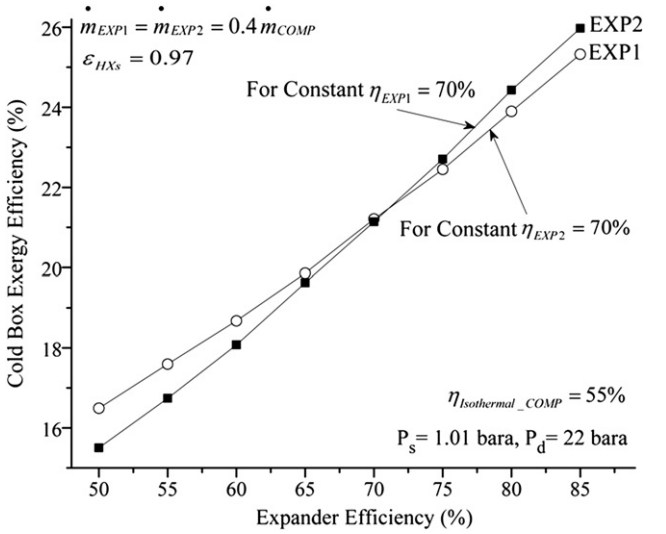

Fig. 9. Effects of variation of expander efficiency on the cold box exergy efficiency [P_s = 1.01 bara, P_d = 22 bara, $\eta_{Isothermal\_COMP}$ = 55%, η_{EXP2} = 70%, $\dot{m}_{EXP1} = \dot{m}_{EXP2} = 0.4\dot{m}_{COMP}$, ε_{HXs} = 0.97].

constant at ε_{Hxs} = 0.97. As surface area is added to a heat exchanger, both its First Law and Second Law efficiencies increase and, as a result, exergy destruction decreases.

However, when increasing the heat exchanger surface area, the pressure drop in HXs increases, which adversely affects the cold box exergy efficiency. The relationship between the increase in heat exchanger size and pressure drop has been shown in Appendix I. In order to understand the impact of pressure drop, heat exchanger surface area or UA addition has been analyzed for two cases; i) without PD (pressure drop) and ii) with PD in both HP and LP lines. For studying the second case, it is assumed that there is a total pressure drop of 0.4 bara in the HP line and 0.2 bara in the LP line which are realistic values for practical plants [38–40]. The total pressure drop in both HP and LP lines are apportioned among the heat exchangers. When increasing UA of a heat exchanger, the pressure drops in HP and LP streams are increased proportionally from their respective base values (at effectiveness of 0.97, the base non-dimensional effective UA values are 17.0, 4.3, 6.9, 1.4 and 1.1 for HX1, HX2, HX3, HX4 and HX5 respectively).

The addition of surface areas to heat exchangers has been performed in terms of non-dimensional effective UA and the results have been plotted in Fig. 10.

The following observations may be made from Fig. 10:

- Adding UA to HX1 has the most prominent effect on cold box exergy efficiency. This is true for both with PD and without PD cases. Addition of UA to HX3 also has quite a significant influence on the exergy efficiency, though it is less in magnitude than that of HX1. It may be reiterated that HX1 and HX3 are the two heat exchangers that determine the inlet temperature to expanders EXP1 and EXP2 respectively.
- When arranging according to the order of influence, HX1 is followed by HX3, HX2, HX4 and finally HX5. This is true for both with PD and without PD cases.
- When pressure drop in heat exchanger is not considered, the cold box exergy efficiency gets saturated when the sizes (surface area) of the heat exchangers exceeds certain value. This value has been termed as saturation effective UA. The saturation UA for HX1 is three times its base value; whereas for HX3, it is at about 1.5 times its base value. For other HXs, however, the increase is much less.

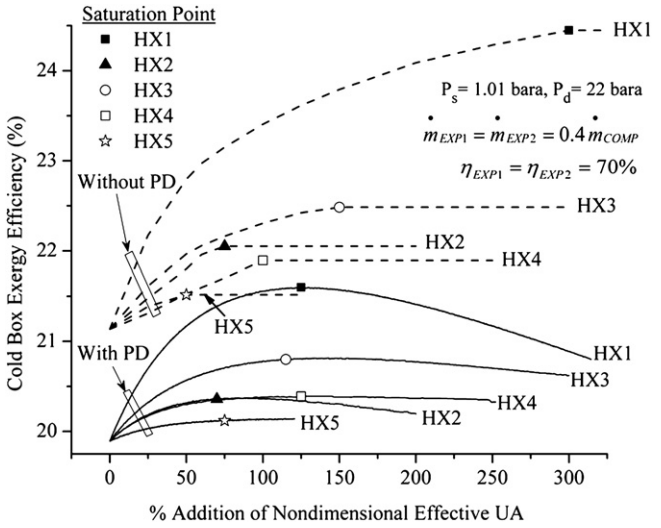

Fig. 10. Effect of percentage addition of non-dimensional effective UA on cold box exergy efficiency [P_s = 1.01 bara, P_d = 22 bara, η_{COMP} = 55%, $\eta_{EXP1} = \eta_{EXP2}$ = 70%, $\dot{m}_{EXP1} = \dot{m}_{EXP2} = 0.4\dot{m}_{COMP}$, base non-dimensional effective UA: HX1: 17, HX2: 4.3, HX3: 6.9, HX4: 1.4 and HX5: 1.1].

- When considering pressure drop, the exergy efficiency initially increases with UA addition. However, it decreases beyond a particular magnitude of UA and the configuration has a maximum efficiency at an optimum UA. For all heat exchangers, exergy efficiency decreases beyond the optimum value; however, for smaller heat exchangers, HX4 and HX5, the drop in exergy efficiency is not significant after it reaches the optimum value.
- For cases where the PD is considered, as expected, the cold box exergy efficiency is less than that without PD. However, the relative effects of heat exchangers on the exergy efficiency with addition of effective UA remain the same whether PD is considered or not.
- The influence of pressure drop is highly significant on the optimum UA values for the bigger heat exchangers HX1 and HX3. For HX1, the optimum UA with PD is 60% less than that of the saturation value of UA without considering PD; for HX3, it is about 20% less. For HX2, the optimum UA value is almost the same as the saturation UA value.
- As PD is taken into consideration, the optimum UA values of the lower temperature heat exchangers HX4 and HX5 slightly increases. It may be due to the fact that when PD is taken into consideration, the liquid production decreases and therefore, the return stream flow through the HXs increases. This would considerably reduce the mass flow imbalance in lower temperature heat exchangers. Therefore, when pressure drop is taken into reckoning, HX4 and HX5 becomes more balanced and they require more UA to reach the optimum conditions.
- There are indications that the sizes of the heat exchangers at higher temperatures feeding to the expanders may be overestimated if saturation UA values are taken as their optimum sizes. However, the magnitude of this overestimation would decrease sharply as relatively lower temperature heat exchangers are considered. If simulations are performed without considering the effect of pressure drop, there may be about 15% overestimation in the contribution of heat exchangers in cold box efficiency. For the case of large-scale liquefiers which involve a higher number of heat exchangers, ignoring the pressure drop would reduce the complexity in simulation process to a great extent. Results show that the results of simulation of a cycle without considering pressure drop may be good enough for the purpose of comparison of performances between different options. However, it may be good enough to use the saturation values of the heat exchanger effective UA only as the initial guess values in simulation.

4. Conclusions

The following conclusions may be drawn from the exergy analysis:

- Compressor discharge pressure should be kept between 18 and 22 bara for helium liquefaction cycles.
- 80% of the compressor flow should be diverted through the expanders for highest performance of helium liquefiers.
- Total expander flow should be equally divided among the expanders to obtain maximum liquefaction.
- Higher efficiencies should be sought for all the expanders irrespective of their operating temperatures.
- It is more important to increase the size (from their base values) of those heat exchangers that determine the inlet temperature to expanders close to their optimum UA in order to get significant improvement in rate of liquefaction.

These conclusions are identical to those already drawn with energy analysis, as available in the literature. It proves the authenticity of the analytical tool of exergy analysis in determining performance of helium liquefiers. However, exergy based analysis allows more conclusions to be drawn, as given below:

- The exergy flow diagram or the Grassmann diagram gives a visual representation of exergy utilization as well as its loss in the cycle. It can therefore be used to provide directions to improve components as well as the cycle.
- Calculation of exergy loss in heat exchangers provided more insight into the temperature profiles of the streams and suggested ways to make heat exchangers more balanced and more effective so as to reduce exergy destructions in them.
- Pressure drop influences the optimum effective UA values of high temperature heat exchangers feeding to the expanders more than those of lower temperature ones, though its impact on the overall cycle efficiency may not be significant.
- Calculations without considering pressure drop in the heat exchangers may be good enough for comparing different cycles and components.
- Values of optimum effective UA with pressure drop for heat exchangers at higher temperatures (leading to the expanders) are less than that of their saturation values without pressure drop. The difference, however, reduces sharply as the operating temperature reduces. The pressure drop reduces the exergy efficiency of the system.
- Exergy analysis is more holistic in approach than the energy analysis in the sense that it can calculate the effect of pressure drop along with other thermal parameters. The performance of Joule-Thomson valve also may be compared with other components with the aid of Second Law, which is otherwise not possible with any of the First law based tools.

It may be concluded that the exergy analysis is capable of drawing more conclusions than offered by the First Law based energy analysis and thereby provides a better and deeper understanding of the process. The major conclusions arising out of the study may help in designing large-scale helium liquefaction cycles. The results would be applicable to plants of any capacity because all the independent and dependent parameters are presented in non-dimensional terms.

Acknowledgment

Financial assistance by Institute of Plasma Research (IPR) at Gandhinagar through a project under National Fusion Programme (NFP) is gratefully acknowledged.

Appendix I

Heat transfer and flow friction for a heat exchanger may be correlated as:

$$\frac{G_{side}^2}{2\rho_{avg}\Delta P_{side}} = \frac{j/f}{\mathrm{Pr}_{avg}^{2/3} NTU_{side}} \tag{A1}$$

where, ΔP_{side} is the pressure drop in one side of heat exchanger, the Colburn factor j represents the characteristic heat transfer coefficient and f is the Fanning friction factor.

The mass velocity, G_{side} which is defined as mass flow rate ($\dot{m}$) per unit cross sectional area (A_c) of one side of the heat exchanger, is expressed as:

$$G_{side} = \frac{\dot{m}_{side}}{A_c} = \rho_{avg} V_{avg} \tag{A2}$$

where, $\dot{m}$ is the mass flow rate, ρ_{avg} and V_{avg} are the average density and velocity of stream respectively at one side of heat exchanger.

Prandtl number Pr_{avg} is the non-dimensional ratio of momentum diffusivity to thermal diffusivity. The average of Prandtl number is written as:

$$\mathrm{Pr}_{avg} = \frac{\mu_{avg} c_{p\_avg}}{k_{avg}} \tag{A3}$$

The Number of Heat Transfer Units for one side NTU_{side} is defined as:

$$NTU_{side} = \frac{hA_s}{\dot{m}_{side} c_{p\_avg}} \tag{A4}$$

where, h represents the convective heat transfer coefficient for one side, A_s is the heat transfer surface area and c_{p_avg} is the average specific heat of the stream at the selected side of heat exchanger.

Eq. (A1) may be re-written as:

$$\Delta P_{side} = \frac{NTU_{side} \mathrm{Pr}_{avg}^{2/3} G_{side}^2}{2(j/f)\rho_{avg}} \tag{A5}$$

The thermal resistance equation for a heat exchanger is written as:

$$\frac{1}{UA} = \frac{1}{(hA_s)_1} + \frac{x}{kA_s} + \frac{1}{(hA_s)_2} \tag{A6}$$

where, x represents the thickness of the parting sheet between hot and cold stream of heat exchanger. Considering that the metal thermal conductivity, k is very high and assuming that $(hA_s)_1=(hA_s)_2$, NTU_{side} given in Eq. (A4) can be written in terms of the product of the overall heat transfer coefficient U and heat transfer surface area A as:

$$NTU_{side} = \frac{2UA}{\dot{m}_{side} c_{p\_avg}} \tag{A7}$$

Substituting Eq. (A7) in Eq. (A5):

$$\Delta P = \frac{(UA)\mathrm{Pr}_{avg}^{2/3} G_{side}^2}{\dot{m}_{side} c_{p\_avg} (j/f) \rho_{avg}} \tag{A8}$$

$$\Delta P = \frac{(UA)\mathrm{Pr}_{avg}^{2/3} \dot{m}_{side}}{A_c^2\, c_{p\_avg} (j/f) \rho_{avg}} \tag{A9}$$

As, $(j/f) = 0.2$ *to* 0.3 for most compact surfaces under turbulent flow conditions for Reynolds number, $Re > 2000$ [41] and considering that within a heat exchanger, for small variations in stream inlet temperatures, the changes in average fluid properties like ρ_{avg},c_{p_avg} and Pr_{avg} are negligible, then it can be written that:

$$\Delta P \propto (UA) \times \dot{m}_{side} \tag{A10}$$

Therefore, it may be concluded that on increasing the (UA) of an heat exchanger there will be proportional increase in pressure drop ΔP for streams on both sides of the heat exchanger, provided the changes in mass flow rates are negligible.

References

[1] Collins SC. A helium cryostat. Rev Sci Instru 1946;18(3):157–67.
[2] Onnes HK. Experiments on the condensation of helium by expansion. KNAW Proc 1907-1908;10(II):744–7.
[3] Ergenc S. Process for liquefaction of helium by expansion. US Patent 1968:3:389–565.
[4] Collins SC. Apparatus for liquefying a cryogen by isentropic expansion. US Patent 1975;3,864,926.
[5] Quack H. Refrigerating plant using helium as a refrigerant. US Patent 1977;4,048,814.
[6] Toscano WM. Helium liquefaction plant.US Patent 1981;4,267,701.
[7] Thomas RJ, Ghosh P, Chowdhury K. Thermodynamic analysis of collin's cycle: aspects of designing large scale helium liquefiers. Presented Int Cryog Eng Conf 23, Wroclaw, July 19-21, 2010.
[8] Thomas RJ, Ghosh P, Chowdhury K. Role of expanders in helium liquefaction cycles: parametric studies using Collins cycle. Fusion Eng Design 2011;86: 318–24.
[9] Thomas RJ, Basak S, Ghosh P, Chowdhury K. Helium liquefaction/refrigeration system based on Claude cycle: a parametric study, presented at the 22nd National Symposium on cryogenics, Indian Institute of Science, Bangalore, December 4-6, 2008. Indian J Cryog 2009;34(1–4):33–8.
[10] Van der Ham LV, Kjelstrup S. Exergy analysis of two cryogenic air separation processes. Energy 2010;35:4731–9.
[11] Yu J, Tian G, Xu Z. Exergy analysis of Joule–Thomson cryogenic refrigeration cycle with an ejector. Energy 2009;34:1864–9.
[12] Remeljej CW, Hoadley AFA. An exergy analysis of small-scale liquefied natural gas (LNG) liquefaction processes. Energy 2006;31:2005–19.
[13] Chiu C, Newton CL. Second law analysis in cryogenic processes. Energy 1980; 5:899–904.
[14] Ahern JE. Applications of the second law of thermodynamics to cryogenics- A review. Energy 1980;5:891–7.
[15] Trepp C. Refrigeration systems for temperatures below 25°K with turbo-expanders. Adv Cryog Eng 1962;7:251–61.
[16] Thirumaleshwar M. Exergy method of analysis and its application. Cryogenics 1979;19(6):355–61.
[17] Matsubara Y, Kaneko M, Hiresaki Y, Yasukochi K. Exergy analysis of multi-staged Claude cycle helium refrigerator. In: Proc of cryog pros and equip in energy sys con. San Fransisco: ASME; Aug 1980. p. 131–4.
[18] Ziegler BO. Second law analysis of the helium refrigerators for HERA proton magnet ring. Adv Cryog Eng 1986;31:693–8.
[19] Ziegler B, Quack H. Helium refrigeration at 40 percent efficiency. Adv Cryog Eng 1992;37:645–51.
[20] Lohlein K, Fukano T. Exergy analysis of refrigerators for large scale cooling systems. Fusion Eng Design 1993;20:511–8.
[21] Hubbel RH, Toscano WM. Thermodynamic optimization of helium liquefaction cycles. Adv Cryog Eng 1980;25:551–62.
[22] Caillaud A, Crispel S, Grabie V, Delcayre F, Aigouy G. Evolution of the standard helium liquefier and refrigerator range designed by Air Liquide DTA, France. Adv Cryog Eng 2008;53:830–7.
[23] McCarty RD, Arp VD. A new wide range equation of state for helium. Adv Cryog Eng 1990;35:1465–75.
[24] Dutta R, Ghosh P, Chowdhury K. Customization and validation of a commercial process simulator for dynamic simulation of helium liquefier. Energy 2011;36(5):3204–14.

[25] Dutta R, Thomas RJ, Ghosh P, Chowdhury K. Dynamic simulation of large-scale helium liquefier using Aspen Hysys®. In: 23rd National Symposium on cryogenics. Rourkela, India: NIT; Oct 28-30, 2010.
[26] Deschildre C, Barraud A, Bonnay P, Briend P, Girard A, Poncet JM, et al. Dynamic simulation of an helium refrigerator. Adv Cryog Eng 2008;53: 475–82.
[27] Ganni V. Optimal design and operation of helium refrigeration systems. Proc of Particle Acc Con PAC09. Vancouver, BC: Canada; May 4-8, 2009.
[28] Barron RF. Cryogenic systems. 2nd ed. New York: Oxford university press; 1985.
[29] Thomas RJ, Ghosh P, Chowdhury K. Exergy analysis of helium liquefaction systems based on modified Claude cycle with two-expanders. Cryogenics 2011;51(6):287–94.
[30] Ganni V, Knudsen P, Creel J, Arenius D, Casagrande F, Howell M. Screw compressor characteristics for helium refrigeration systems. Adv Cryog Eng 2008;53:309–15.
[31] Bejan A, Tsatsaronis G, Moran M. Thermal design and optimization. Ist ed. New York: John Wiley & Sons; 1996.
[32] Kotas TJ. The exergy method of thermal plant analysis. 1st ed. London: Butterworths; 1985.
[33] Asakura H, Saji N, Yoshinaga S, Ishizawa T, Ikeuchi M, Yanagi H. Development of a highly reliable helium refrigeration system-R&D of a highly reliable helium refrigeration system (oil-free type). Cryogenics 2002;42:203–8.
[34] Yamada S, Satoh S, Mito T, Maekawa R, Iwamoto A, Moriuchi S, et al. Liquefaction control of 10kw class cryogenic system for the LHD. Proc ICEC 16/ICMC 1996;16:83–6.
[35] Bai H, Bi Y, Zhu P, Zhang Q, Wu K, Zhuang M, et al. Cryogenics in EAST. Fusion Eng Design 2006;81:2597–603.
[36] Gruehagen H, Wagner U. Measured performance of four new 18 kW @ 4.5 K helium refrigerators for the LHC cryogenic system. Proc ICEC 2005;20: 991–4.
[37] Choi CH, Chang HS, Park DS, Kim YS, Bak JS, Lee GS, et al. Helium refrigeration system for the KSTAR. Fusion Eng Design 2006;81:2623–31.
[38] Ergen C, Trepp Ch. A large-scale helium liquefier. Sulzer Tech Rev 1966;4:1–4.
[39] Toscano WM, Kudirka FJ. Thermodynamic and mechanical design if the FNAL central helium liquefier. Adv Cryog Eng 1976;21:456–66.
[40] Cammarata G, Fichera A, Guglielmino D. Optimization of a liquefaction plant using genetic algorithms. App Energy 2001;68:19–29.
[41] Hesselgreaves JE. Compact heat exchangers: selection, design, and operation. Kidlington, UK: Pergamon Press; 2001.